

SILAGE PRESSURES IN TOWER SILOS. PART 2. MEASUREMENT OF PHYSICAL PROPERTIES AND EFFECT OF SILO CHARACTERISTICS

S.C. Negi, J.R. Ogilvie, and E.R. Norris

Agricultural Engineering Department, Macdonald College of McGill University, Ste. Anne de Bellevue, Quebec

Received 23 December 1975

Negi, S.C., J.R. Ogilvie, and E.R. Norris. 1977. Silage pressures in tower silos. Part 2. Measurement of physical properties and effect of silo characteristics. *Can. Agric. Eng.* 19: 98-106.

Laboratory data on effective yield loci of silage materials and wall yield loci of silage and some structural surfaces are obtained and the salient features of these data are emphasized. Computed results are presented to illustrate the effects of wall friction and silo diameter on the magnitude and distribution of silage pressures in tower silos.

INTRODUCTION

There is a need for quantitative information on the physical properties of silage materials that affect the pressure distribution in storage structures. The relevant factors are silage density, internal friction properties of silage and the wall friction characteristics. The density and the internal friction properties of silage depend on the type of silage material, the length of cut, maturity of the crop, moisture content and depth of silage. The wall friction characteristics are influenced by the degree of roughness of the wall surface, moisture content of both the material and the surface, material characteristics and environmental conditions.

The approach adopted in this study for determination of the aforementioned physical properties is based on the yield locus concept due to Jenike and Shield (1959).

The strength of a bulk solid can be represented graphically in the normal pressure-shearing stress coordinates by a line called the yield locus, YL. For a material in the state of plastic equilibrium and at the point of incipient failure, the stresses can then be represented by a Mohr circle just touching the material yield locus (Jenike 1964; Walker 1966).

The position of the yield locus is a function of the density of the material. As the density or the degree of consolidation increases, the yield locus expands, terminating at the point of tangency of the Mohr circle. Stresses beyond the terminal point cannot be applied without increasing the density of the material and shifting to a new yield locus (Jenike et al. 1960). Consequently, for a compressible and cohesive material like silage, a family of yield loci exists, each locus terminating at the stress conditions corresponding to its density (Walker 1966). The envelope of the terminal Mohr circles of each yield locus is defined as the effective yield locus, EYL, and the slope of this common tangent is called the effective angle of internal friction, ϕ (Jenike 1964). It has been found experimentally that even for a cohesive material, the effective yield locus is approximately linear and passes through the

origin (Walker 1966).

The limiting stress conditions that can be sustained at the interface between the stored material and container wall are represented on a normal-shearing stress diagram by a line called the wall yield locus, WYL (Jenike 1964; Walker 1966). The slope of the wall yield locus is the wall friction angle, δ .

This paper is concerned with the determination of the effective yield loci of silage, and the wall yield loci of silage and the structural surfaces commonly used for construction of tower silos. Laboratory data on the effective angle of internal friction and the angle of wall friction are obtained at various moisture levels to cover the range in which

silage materials are normally held in storage. Further, the relative importance of the effects of some pertinent variables on the magnitude and distribution of silage pressure components in a tower silo are evaluated.

MATERIALS AND METHODS

Sample Materials

The silage materials used in this study were collected from tower silos in current use at the Macdonald College Farm. Corn and grass silage samples were tested roughly 6 and 9 mo, respectively, after the loading of the fresh materials. In both cases, the

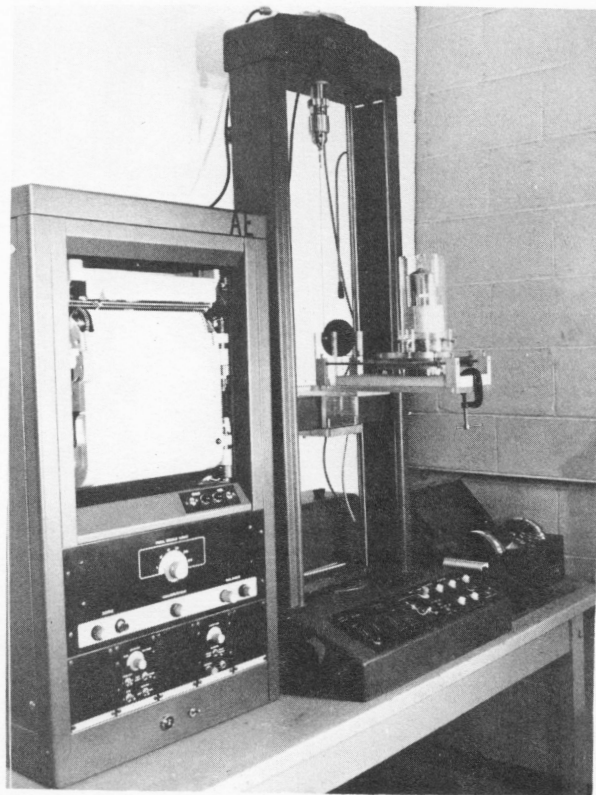


Figure 1. Instron machine with friction attachment.

theoretical length of cut was 0.6 cm. The moisture content of corn silage averaged 67.7% on a wet basis. Grass silage containing approximately 50% alfalfa and 50% bromegrass was at 68.2% moisture content when acquired. For moisture determinations, silage samples were dried for 24 h in an electric air oven at 105 ± 2 C. Tests for internal and wall friction properties were conducted with corn silage at 79.1, 67.7 and 56.9% moisture; and with grass silage at 77.6, 68.2, 57.5 and 45.1% moisture. The different levels of moisture were obtained by either drying or rewetting the silage material. The silage was then thoroughly mixed and stored in sealed plastic bags for at least 48 h, so the moisture would reach an equilibrium. Several samples were taken and oven-dried to determine the final moisture content.

The surfaces chosen for wall friction tests were (i) galvanized steel, (ii) concrete stave, (iii) steel trowel finish concrete, and (iv) pine wood stave. These materials were considered to represent the wall surfaces of the more commonly used tower silos.

Internal Friction Properties

The equipment used to determine the effective angle of internal friction ϕ included a direct shear apparatus and a packing mold. The shear cell utilized a 5.1-cm square box divided horizontally into two halves. Normal loads were applied through a counterbalanced weight hanger system. The shearing force was applied by a hand crank operating through a gear system. Shearing forces were measured by a 110-kg capacity single proving ring assembly. The packing mold consisted of a hollow square metal box with an inverted L-shaped groove at the bottom to fit the shear cell.

The test method consisted of preparing a uniformly packed sample of silage and subjecting it to a shear-consolidation operation under a preselected normal load. The specimen was then sheared under another smaller normal load. From a set of such tests, a yield locus of shear force versus normal load was plotted and a Mohr semicircle was drawn tangential to the yield locus and passing through the point determined by the shear-consolidation procedure. A tangent to the Mohr semicircle was also drawn through the origin to obtain the effective yield locus and the slope of this tangent determined the effective angle of friction ϕ . Jenike (1964) gives a detailed description of the experimental procedure.

Wall Friction Characteristics

The angle of friction δ between silage and a silo wall material was measured on a specially constructed apparatus attached to a testing machine (Instron Universal Model TM-M) as shown in Fig. 1. The friction apparatus, similar to that developed by Clark and McFarland (1973), is shown in Fig. 2. A cast acrylic sample cylinder, 9.5 cm inside diam, was fitted into a 15.3-cm square

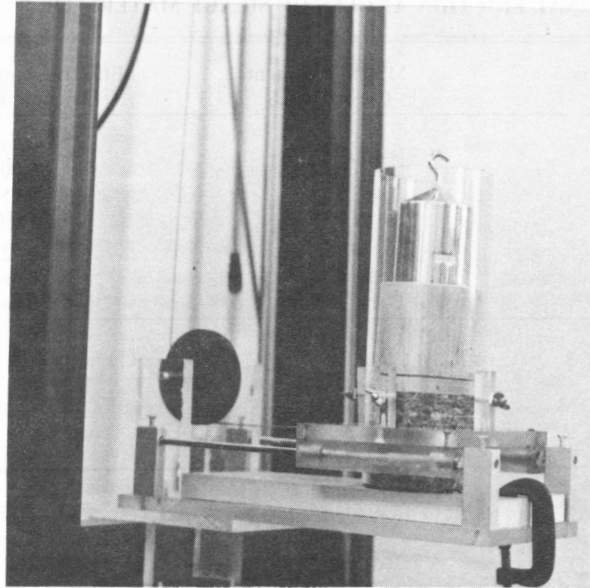


Figure 2. Wall friction apparatus.

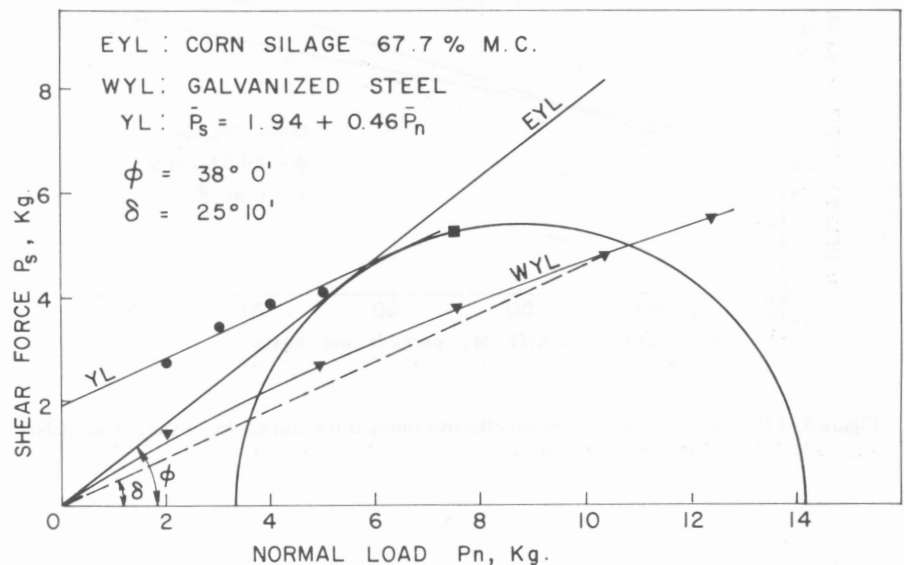


Figure 3. Effective yield locus of corn silage at 67.70% moisture content.

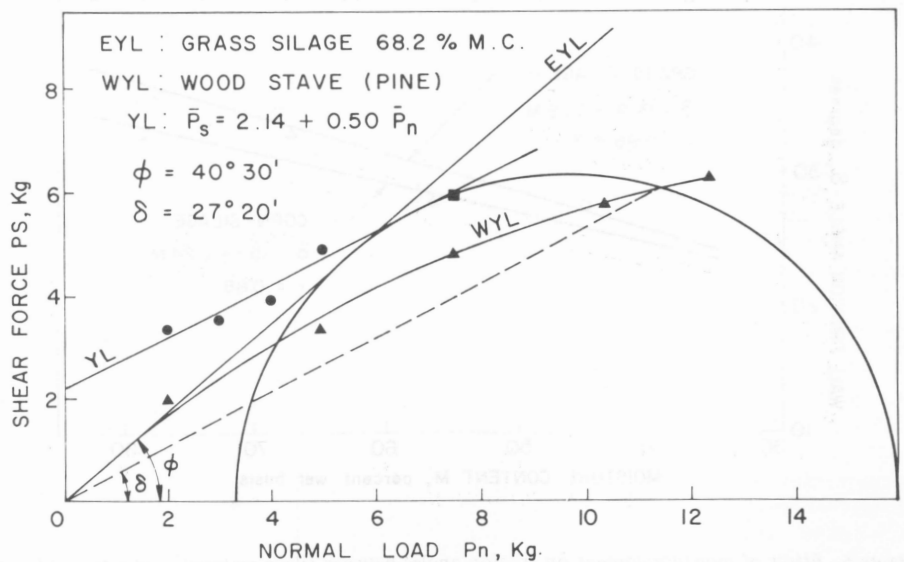


Figure 4. Effective yield locus of grass silage at 68.20% moisture content.

TABLE I INTERNAL FRICTION ANGLES OF SILAGE MATERIALS

Type of silage material	Moisture content (% wet basis)	Effective angle of internal friction (radians)
Grass silage (alfalfa 50%, brome-grass 50%)	77.6	0.7985
	68.2	0.7068
	57.5	0.6515
	45.1	0.6065
Corn silage	79.1	0.7243
	67.7	0.6632
	56.9	0.6428

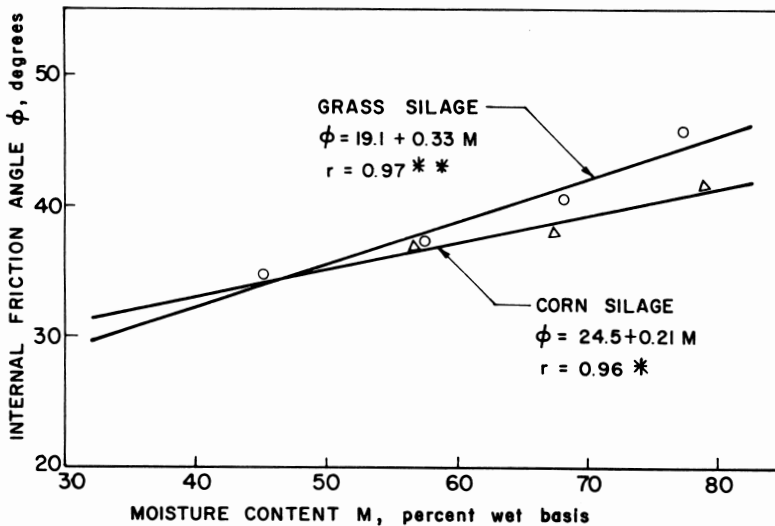


Figure 5. Effect of moisture content on effective internal friction angles of silage materials.

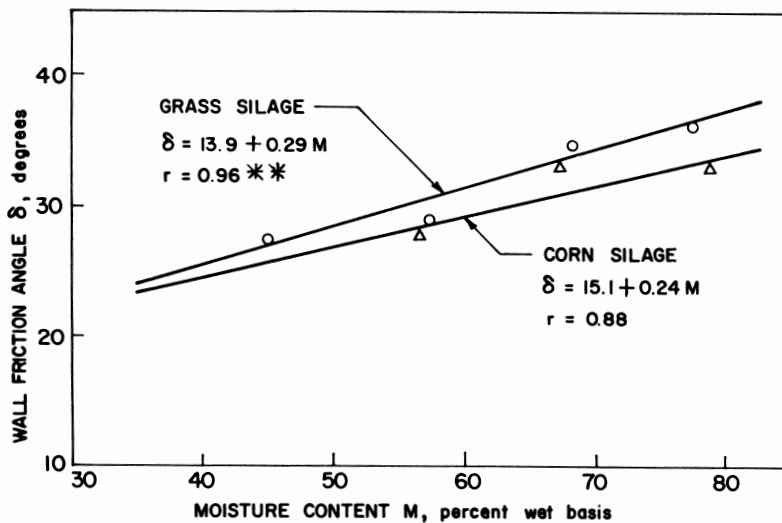


Figure 6. Effect of moisture content on friction angles between silage materials and a trowel-finish concrete surface.

platform. The cylinder mount was attached to two bearing blocks, one on either side. These blocks contained linear bearings sliding on polished steel guide rails fixed to the apparatus base. The base of the apparatus was mounted on the crosshead of the testing machine. The sample container was connected by a stranded wire cable passing over a pulley to the tension load cell of the machine.

In conducting a test, the sample of the wall material was clamped to the base of the friction apparatus. A specimen of silage material to be tested was weighed and placed in the cylinder. The silage was slightly compacted, leveled and covered by a rigid plate to assure uniform load distribution across the specimen. Five machined iron weights were placed on top of the loading plate to give the largest necessary normal load. The weight of the silage sample, loading plate and the surcharge weights determined the normal loads P_n . The cylinder was raised slightly above the test surface and clamped by adjusting screws against four square stocks fastened to the platform. Thus the total superimposed load was transferred directly on the interface between silage and wall surface material.

The horizontal force required to pull the sample container over the test surface was continuously recorded. A crosshead speed of 0.5 cm/min was used in all tests. Since the cylinder mount friction was very small, the force registered on the recorder chart was used directly as the friction force. When the friction force, P_s , leveled off, one weight was removed; and after a while, when P_s again leveled off, another weight was removed. This procedure was repeated until a steady friction force for the last surcharge weight was obtained.

Five replications were made with each combination of moisture level, silage, and wall surface material. The mean friction forces corresponding to normal loads of 12.35, 10.35, 7.52, 4.92 and 2.00 kg were plotted in the P_n, P_s system of coordinates. A smooth curve passing through the origin and the plotted points was drawn to obtain the wall yield locus, WYL. The resulting curve was superimposed on the appropriate EYL diagram to locate the point of intersection of WYL with the Mohr semicircle. The slope of the line drawn through this point and the origin determined the wall friction angle, δ .

RESULTS AND DISCUSSION

Frictional Properties

The construction of the effective yield loci, EYL, for corn silage at 67.7% and grass silage at 68.2% moisture content is illustrated in Figs. 3 and 4, respectively. The EYL is defined by the effective angle of friction, ϕ , as shown in the figures. The values of angle ϕ obtained for silage materials at various moisture contents are

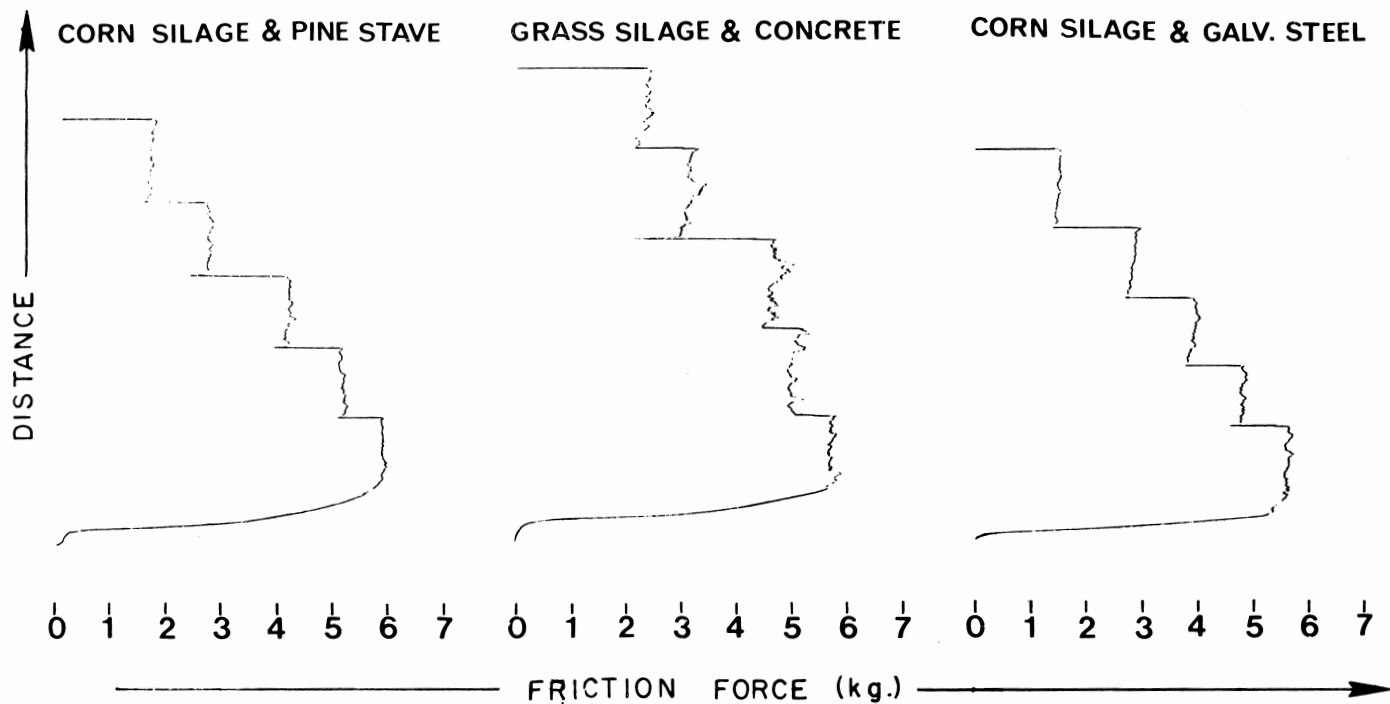


Figure 7. Typical recorder charts — Measurement of WYL. Friction forces (kg) indicated correspond to normal loads of 12.35, 10.35, 7.52, 4.92 and 2.00 kg.

reported in Table I.

For bulk solids that exhibit the properties of granular-cohesive mixtures, it has been found experimentally that the yield loci form a family of convex-upward curved lines (Jenike 1964). The curved yield locus represents changes in the mechanical properties of the mass. As seen in Figs. 3 and 4, the yield loci of silage materials did not form convex-upward curves, but linear regression analyses indicated that straight lines provided reasonable approximations. The scatter in the values of shearing force was ascribed to the inherent geometric inhomogeneities of the test media.

The results of these tests indicate that shearing resistance of silage is due to a combination of internal friction and cohesion. The internal friction is considered to consist of resistance to displacement through interlocking of silage fibers. The cohesion is considered to be the result of bond forces between the silage particles. Since silage mass consists of mixed particle sizes, it is important to differentiate between the coarse particles and the fines insofar as bond forces of an interparticle nature are concerned. The coarse particles, such as parts of stalk, cobs and kernels, are not likely to develop any cohesion. Thus, shear strength of silage due to cohesion arises from binding forces between the finer particles, such as fragments of leaves, tassels and other flaky and fibrous components.

The variation of effective angle of internal friction with moisture content is shown in Fig. 5. The regression equations and correlation coefficients of the resulting curves are presented. Homogeneity of the

TABLE II WALL FRICTION ANGLES (RADIAN)

Type of silage material	Moisture content (% w.b.)	Silo wall surfaces			
		Concrete (trowel-finish)	Galvanized steel	Concrete stave	Wood stave (pine)
Grass silage (alfalfa 50%, bromegrass 50%)	77.6	0.6327	0.4974	0.4581	0.4930
	68.2	0.6065	0.4363	0.4043	0.4770
	57.5	0.5061	0.4145	0.3971	0.4581
	45.1	0.4800	0.4014	0.3752	0.4101
Corn silage	79.1	0.5817	0.4872	0.4349	0.5149
	67.7	0.5760	0.4392	0.3665	0.4887
	56.9	0.4873	0.3752	0.3549	0.4232

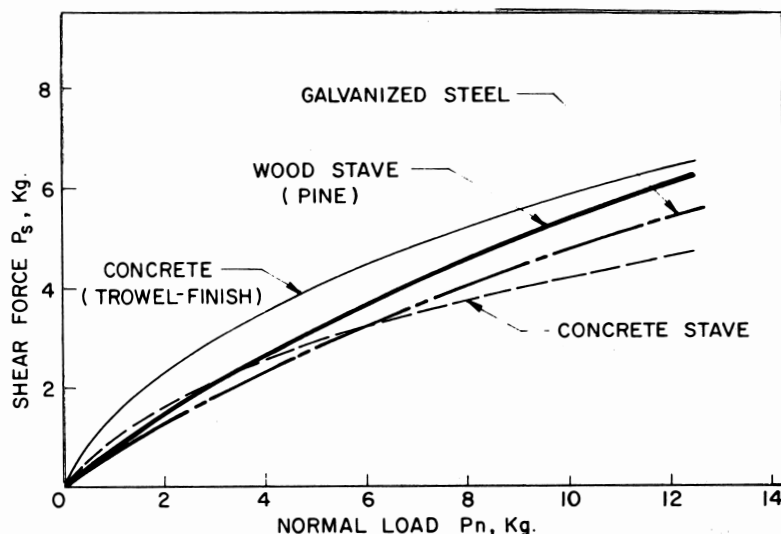


Figure 8. Wall yield loci of corn silage at 67.7% moisture content.

regression coefficients tested by an appropriate F-test in an analysis of covariance revealed that the slopes of the linear regression curves are not significantly different at the 5% level for the two silage materials. That is to say that the two lines have the same slope but not that they are the same line. To decide the effect of the treatments, adjusted means were tested. The analysis indicated that the two lines do not differ significantly at the 5% level. Therefore, the relationship between effective angle of internal friction ϕ , and moisture content M , of both materials can be described by a single linear regression equation given below.

$$\phi = 21.8 + 0.27 M$$

Reference to Fig. 5 shows that the angle ϕ increased with an increase in the moisture content of the material being tested. It appears that at higher moisture levels the interstices between the silage constituents contain both water and air, and the particles with an adsorbed water film around them are held together by surface tension forces.

Figure 6 shows the effect of moisture content on friction angles between silage materials and a steel trowel finish concrete surface. The values of wall friction angle δ for two silage materials at various moisture contents on four structural surfaces are reported in Table II. It is seen from Fig. 6 and the tabulated data that wall friction angle increased with an increase in moisture content. This is attributed to an increase of adhesion due to the surface tension forces acting on the thin film of water adsorbed on the interface between silage and wall surfaces.

Typical recorder charts for wall yield locus measurements are presented in Fig. 7. It is seen that the friction force developed between the test surface and the silage material increased steadily until the motion was impending. After the peak was reached, the frictional force required to maintain motion fluctuated in the neighborhood of the static friction force. The fluctuations of the kinetic friction force were especially pronounced when the asperity of the test surface increased. For instance, it is noticeable from the recorder charts that for a relatively rough surface, such as concrete, the motion followed the stick-slip pattern; whereas for smoother surfaces, such as galvanized steel and pine wood stave, the sliding was relatively smooth and the stick-slip action was at a minimum.

Typical wall yield loci of four structural surfaces are shown in Figs. 8 and 9 for corn and grass silage, respectively. The influence of surface roughness is manifested by the variance in curvature, shape and position of the yield loci. For example, the curvature of the concrete yield locus is more pronounced at low values of normal load than the curvature of the steel yield locus. Also, WYL of concrete occupies a higher position in the

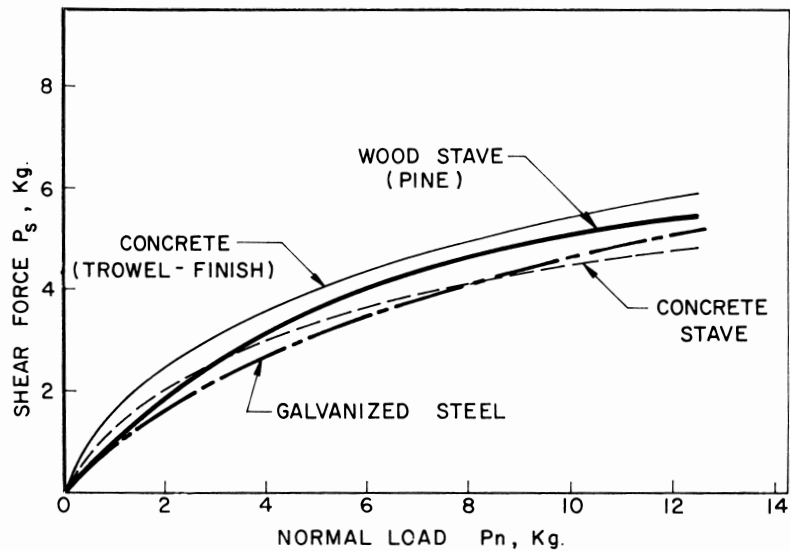


Figure 9. Wall yield loci of grass silage at 57.5% moisture content.

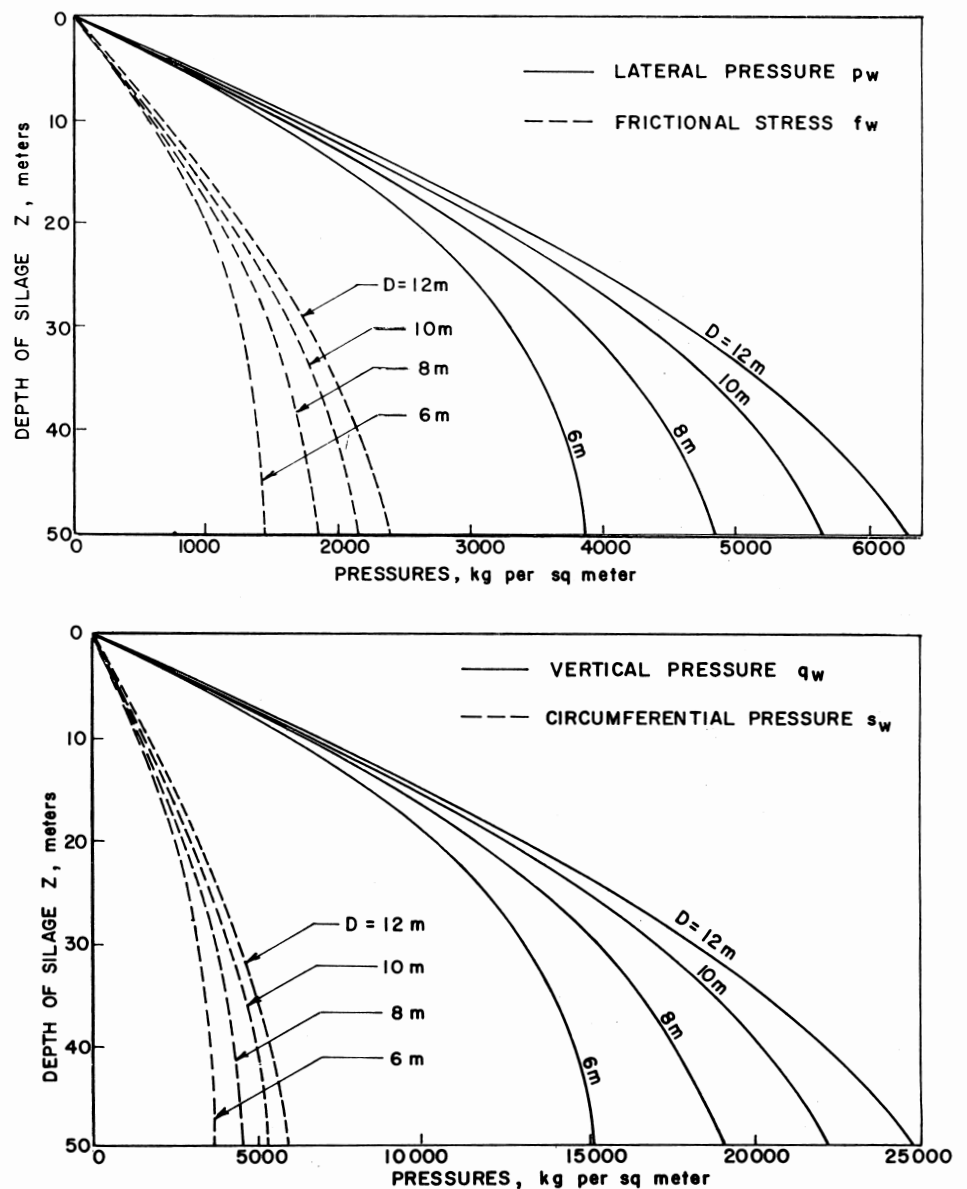


Figure 10. Effect of silo diameter D , active condition (corn silage: $M = 67.7\%$, $\phi = 38^\circ$; concrete stave silo: $\delta = 21^\circ 0'$).

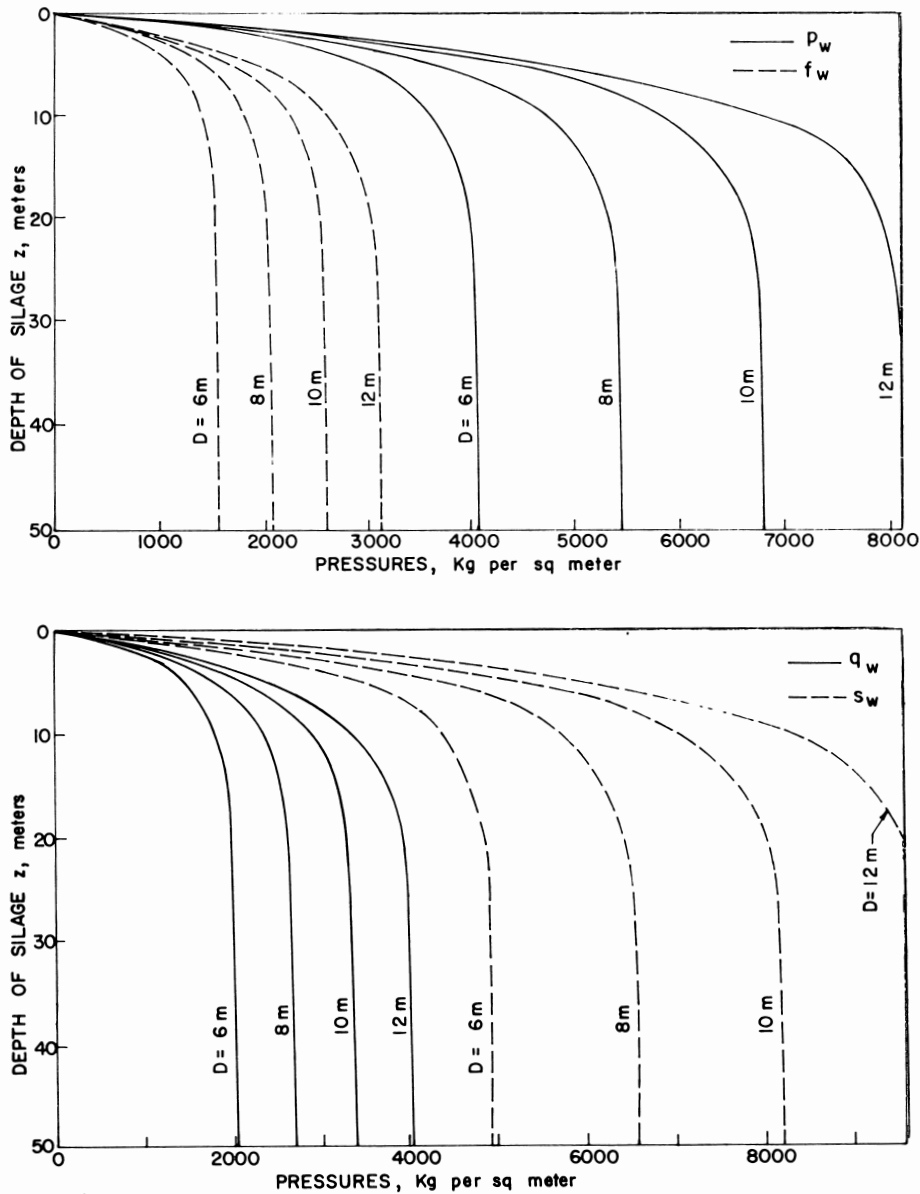


Figure 11. Effect of silo diameter D , passive condition (corn silage: $M = 67.7\%$, $\phi = 38^\circ 0'$; concrete stave silo: $\delta = 21^\circ 0'$).

P_n - P_s diagram than the WYL of steel. This implies that the limiting stress that can be sustained at the boundary wall is greater in a concrete silo than in a steel silo.

Silage Pressure Distributions as Related to Silo Characteristics

In order to assess the relative importance of the factors affecting silage pressures in tower silos, the following results were obtained from the theory presented in Part 1. Due to the lack of experimental data on the variation of silage density with depth in

the 35-65% moisture content range, the effects of the variables ϕ and M could not be investigated. However, the effects of silo diameter and wall friction were examined. This was achieved by selecting a standard set of parameters (corn silage: $M = 67.7\%$, $\phi = 38^\circ$; concrete stave silo: $D = 10$ m, $\delta = 21^\circ$) and then varying each parameter (δ or D) while keeping all others constant.

The effects of silo diameter on the magnitude and distribution of silage pressures are shown in Figs. 10 and 11 for the active and passive conditions, respectively. In general, the magnitude of all pressure

components increases with an increase in silo diameter. This effect is more pronounced at a greater depth in the active case than in the passive. Further, the incremental change in pressure components decreases with increasing diameter in the active case but is essentially independent of the change in diameter in the passive case once the pressures reach their limiting values.

From a comparison of the two cases in Figs. 10 and 11, it is noted that the pressures approach asymptotically the limiting values more rapidly in the passive case than in the active case.

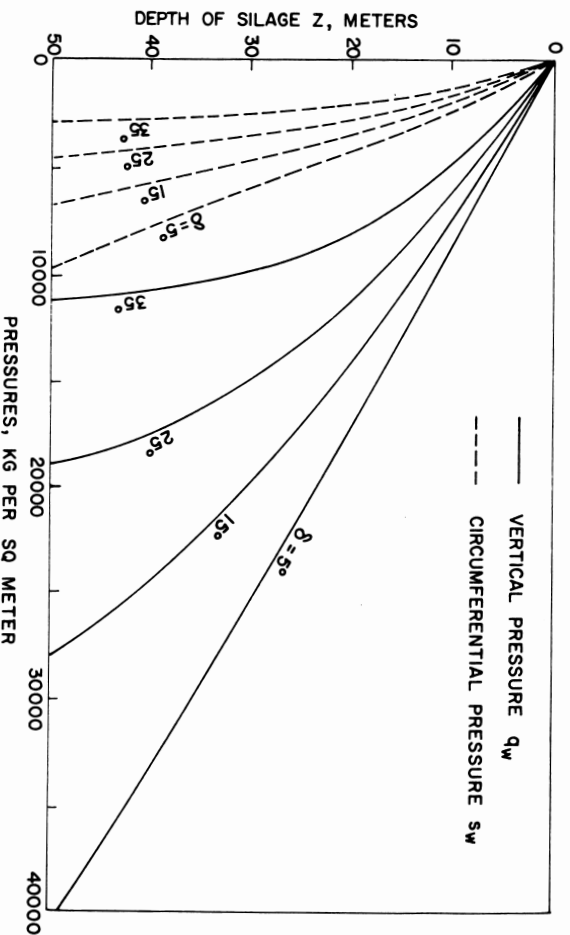
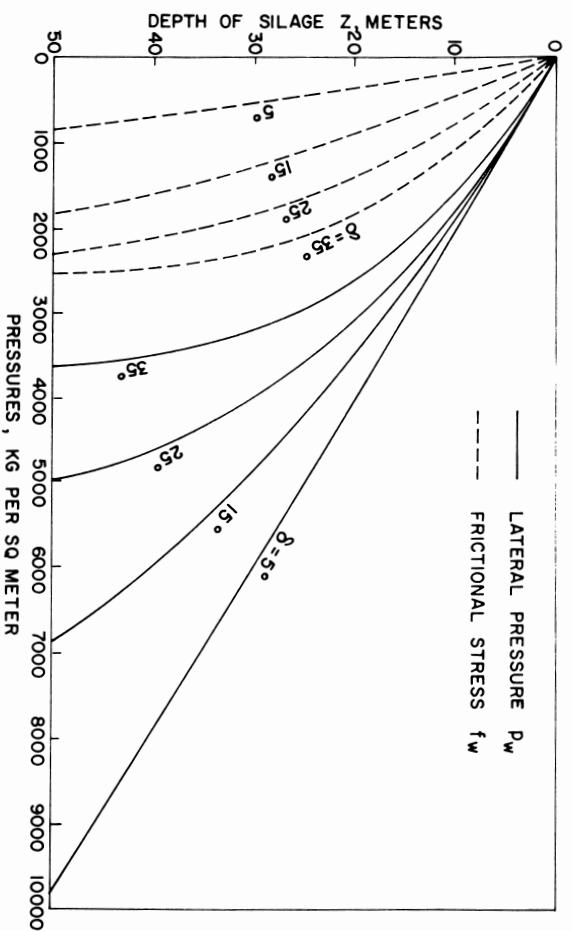


Figure 12. Effect of wall friction angle δ , active condition (corn silage, $M = 67.7\%$, $\phi = 38^\circ 0'$, $D = 10$ m).

The effect of wall friction angle δ on the pressures developed by silage materials at the silo wall in the active case is shown in Fig. 12. The magnitude of vertical (q_w), lateral (p_w) and circumferential (s_w) pressure components increases with smoother walls. Furthermore, the distribution of these pressure components tends towards linearity as the smoothness of the wall increases, or $\delta \rightarrow 0$. As can be expected, the frictional stresses (f_w) developed along the walls attenuate as the smoothness of the wall increases. Also, as $\delta \rightarrow 0$, the frictional stresses approach a linear distribution. Thus, for the case of zero wall friction,

which is not physically possible, an equivalent liquid pressure distribution is developed and the whole weight of the silage mass is transmitted directly to the bottom of the silo. However, for the realistic case of finite wall friction, the weight of the silage material is transferred partly to the walls by friction and partly to the base of the silo. Any change that increases the load carried by the walls reduces the pressure on the base, and vice versa. Consequently, in practice, no unique situation can arise that would produce maximum pressure on the silo walls and the base concurrently.

Figure 13 illustrates the influence of δ

of the magnitude and distribution of silage pressures for the passive condition. The vertical pressure component q_w attenuates with a change in wall friction angle ($\delta = \phi$ to $\delta = \frac{\phi}{2}$). This pressure component q_w increases with a further change in δ ($\delta = \frac{\phi}{2}$ to $\delta \rightarrow 0$).

Likewise, the distribution of the circumferential pressure s_w reaches a low point for a value of $\delta = 0.8 \phi$.

From Fig. 13 it can be seen that the lateral pressure p_w increases whereas the frictional stress f_w decreases with smoother walls. Also, it is noticeable from this figure that frictional stresses are reasonably insen-

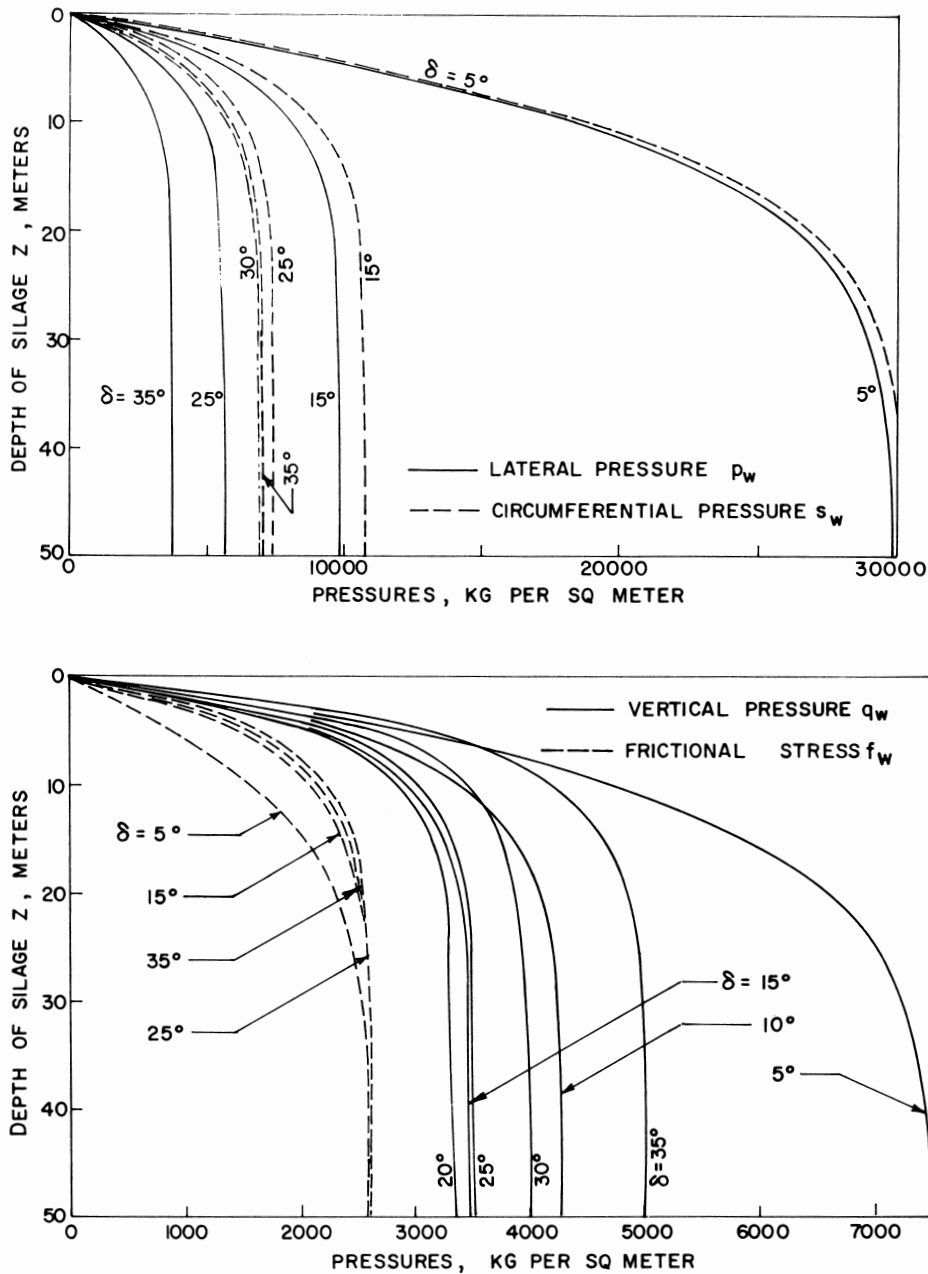


Figure 13. Effect of wall friction angle δ , passive condition (corn silage, $M = 67.7\%$, $\phi = 38^\circ$, $D = 10$ m).

sitive to large variations of δ ($\delta = \phi - 0$) once they reach their limiting values.

Figure 14 shows the variation of q_w with δ in the passive case for four different depth-to-diameter ratios. It is seen that q_w has a minimum value at $\delta = \frac{\phi}{2}$. Physical interpretation of this phenomenon is rather difficult since q_w , among other things, is a function of two independent variables ϕ and δ . The effect of a change in δ , at the boundary wall, and the contribution of ϕ , of the flowing particulate solid, on the behavior of pressure component q_w cannot

be easily visualized.

Although the theoretical results of silage-wall interaction cannot be easily construed in cause-and-effect terms, it is apparent from the preceding discussion that the wall friction angle δ influences the silage pressures considerably. For example, in the active case, the increase in pressure, using a δ of 15° instead of the correct value of 35° and for $\phi = 38^\circ$, gives 51% too high a computed value of wall pressure at the 30-m depth. The importance of incorporating the relevant physical properties into the design formulas cannot be overstated.

- CLARK, R.L. and H.A. McFARLAND. 1973. Granular materials friction apparatus. Amer. Soc. Agric. Eng. Pap. No. 73-544. ASAE, St. Joseph, Mich.
- JENIKE, A.W. 1964. Storage and flow of solids. Utah Eng. Exp. Sta. Bull. 123.
- JENIKE, A.W., P.J. ELSEY, and R.H. WOOLEY. 1960. Flow properties of bulk solids. Proc. Amer. Soc. Test. Mater. 60: 1168-1181.
- JENIKE, A.W. and R.T. SHIELD. 1959. On the plastic flow of coulomb solids beyond original failure. J. Appl. Mech. 27: 599-602.
- WALKER, D.M. 1966. An approximate theory for pressures and arching in hoppers. Chem. Eng. Sci. 21: 975-997.

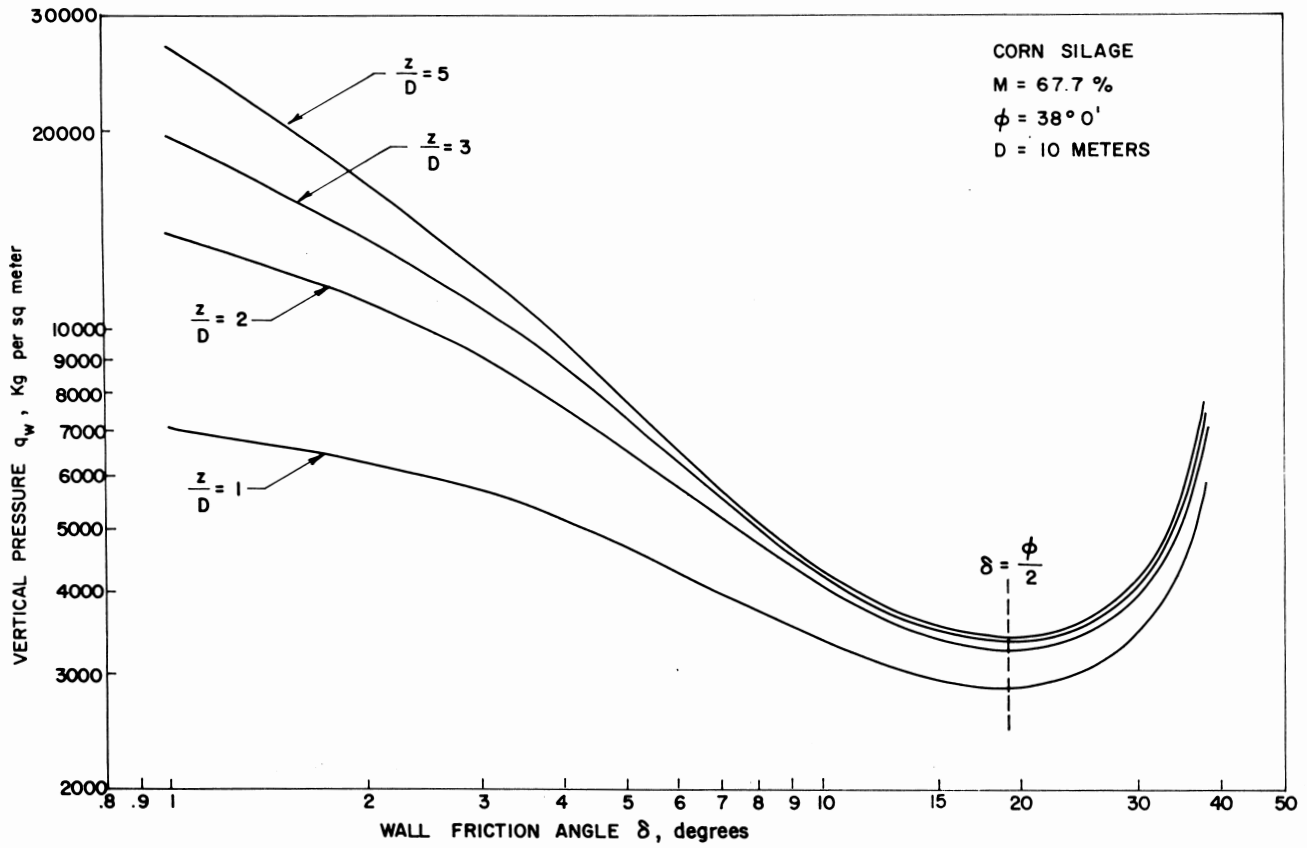


Figure 14. Variation of q_w with δ for different depths of fill, passive condition.